



HAL
open science

Thermochemistry of 1-methylnaphthalene hydroconversion : comparison of group contribution and ab-initio models.

Maria Contreras, Theodorus de Bruin, Pascal Mougin, Hervé Toulhoat

► **To cite this version:**

Maria Contreras, Theodorus de Bruin, Pascal Mougin, Hervé Toulhoat. Thermochemistry of 1-methylnaphthalene hydroconversion : comparison of group contribution and ab-initio models.. *Energy & Fuels*, 2013, 27 (9), pp.5475-5482. 10.1021/ef401064j . hal-00907705

HAL Id: hal-00907705

<https://ifp.hal.science/hal-00907705>

Submitted on 10 May 2022

HAL is a multi-disciplinary open access archive for the deposit and dissemination of scientific research documents, whether they are published or not. The documents may come from teaching and research institutions in France or abroad, or from public or private research centers.

L'archive ouverte pluridisciplinaire **HAL**, est destinée au dépôt et à la diffusion de documents scientifiques de niveau recherche, publiés ou non, émanant des établissements d'enseignement et de recherche français ou étrangers, des laboratoires publics ou privés.



Distributed under a Creative Commons Attribution - NonCommercial 4.0 International License

Thermochemistry of 1-Methylnaphthalene Hydroconversion: Comparison of Group Contribution and *ab Initio* Models

Maria S. Contreras, Theodorus de Bruin, Pascal Mougín, and Hervé Toulhoat*

IFP Energies nouvelles, 1 et 4 avenue de Bois Préau, 92852 Rueil-Malmaison, France

ABSTRACT: As a necessary step in the development of microkinetic models for the hydroconversion of heavy hydrocarbon fractions, we report an assessment of various Density Functional Theory (DFT) models for the calculation of molecular thermochemical properties in comparison with Benson's group contribution method for reactants, intermediates, and products involved in the hydrogenation of 1-methylnaphthalene. The association of the G4 level with homodesmotic decomposition schemes (HI-G4-iso method) has significantly improved the accuracy of the calculated thermodynamic properties when the resemblance of reactants and products is taken into account. Although smaller deviations are observed for Benson's GA method, some limitations appear when position isomers are included. This gap can be fulfilled with homodesmotic/DFT models, whose deviations are not so far from those obtained with Benson's GA method.

INTRODUCTION

To satisfy the increasing global energy demand, it has become mandatory to make better use of heavy crude oils, vacuum residues, bitumen, and asphalts, by cracking these oils and/or cuts into lighter fractions such as gasoline, diesel, and kerosene.¹ Hydrocracking combines the cracking process together with the removal of sulfur, nitrogen impurities, and the saturation of aromatic and unsaturated bonds. To gain more insight in this process, numerous experimental and theoretical studies have been conducted.² However, all these studies are hampered by the large variety of complex chemical structures. Despite a vast body of work on characterization techniques and experimental information on molecular structures of heavy petroleum fractions, the current analytical techniques do not allow characterization of individual molecules or isomer groups in heavy oils. The widely used SARA method of characterization classifies the components of the oil into four big families: saturates, aromatics, resins, and asphaltenes. Aromatics, resins, and asphaltene fractions contain one or several nuclei, or cores, composed of aromatic and/or naphthenic cycles, onto which aliphatic chains are grafted. Since these molecules are very complex, a detailed molecular description is generally not available. Molecular structures of reconstructed aromatic, asphaltene and resin molecules have therefore been proposed.³

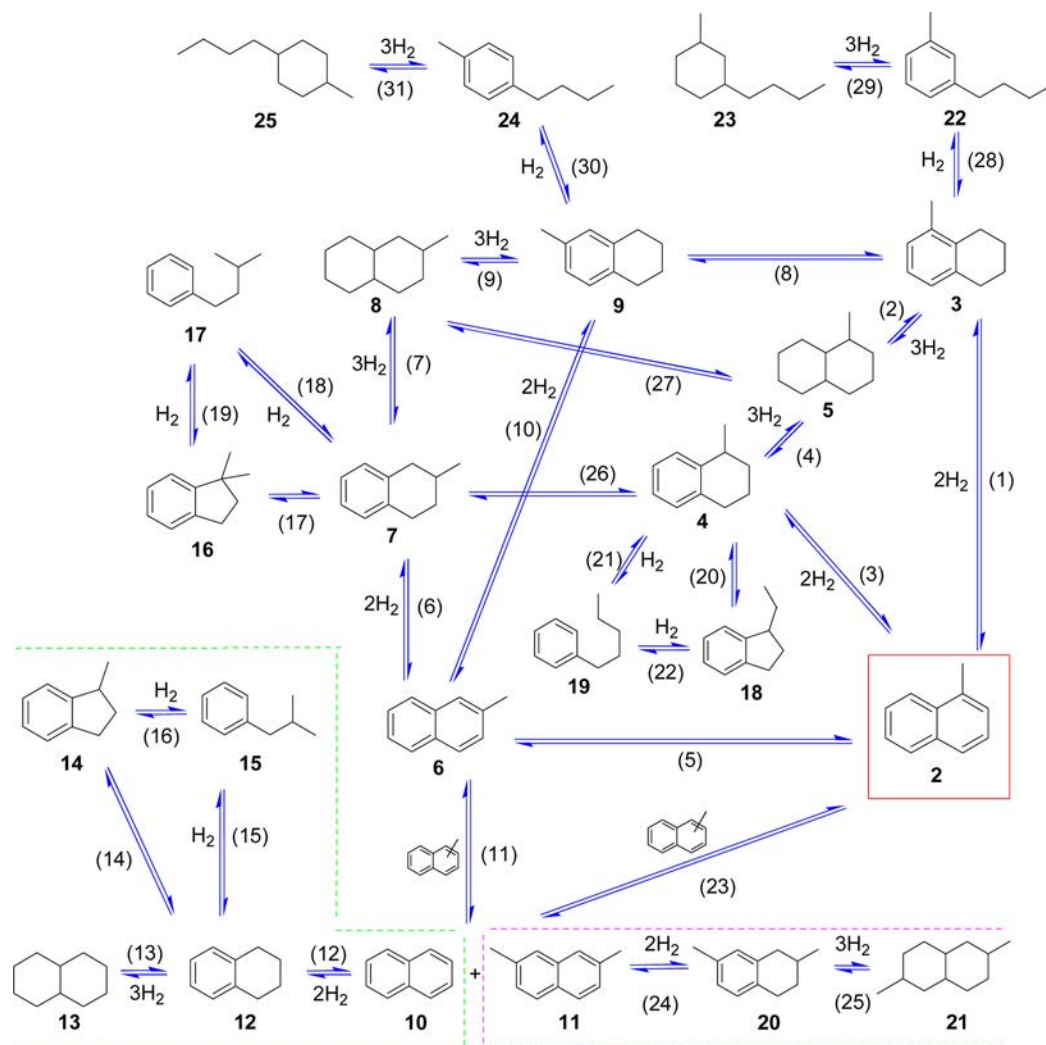
The hydroconversion process is generally carried out at high temperatures (320–380 °C) and H₂ pressures up to 150 bar. These reaction conditions are the result of a compromise between the thermodynamics and kinetics: the thermodynamic equilibrium shifts at lower temperatures to the right in favor of the hydrogenated products, while the reactions become intrinsically faster at higher temperatures. Consequently, to find the optimum reaction conditions, a detailed knowledge of the thermodynamics and kinetics of the elementary reactions for the hydrogenation is mandatory. Once these properties have been determined, microkinetic models can be developed that predict the final product composition. The identification of all

the essential elementary reactions for asphaltene or resin type molecules (or representative models thereof) hydrogenation is an almost impossible task. Instead, we have selected a well-defined model compound, 1-methylnaphthalene (1MN), for which Scheme 1 depicts the most essential hydrogenation reactions. In this scheme, also two cracking reactions are presented: the demethylation of 1MN and the ring-opening reactions of the aliphatic cycle.

In order to model the system as shown in Scheme 1, reaction rates for all direct and reverse reactions must be represented as functions of temperature and H₂ pressure. Since the ratios of direct to reverse rate constants are equal to the equilibrium constants, a useful constraint will be provided by the knowledge of the latter. To that end, it is mandatory to calculate the Gibbs energies of reactants and products. Since experimental data are available only for a limited number of molecules (Table 1) in the literature, we turn to computational methods to complete this data set.

A large body of work has been performed over the past four decades to estimate thermochemical properties of organic compounds. For example, the group additivity (GA) method developed by Benson et al.⁴ allows estimating thermochemical properties like the heat of formation, heat capacity, and entropy, but their accuracy is not guaranteed for any possible structure. Benson's method does not incorporate stabilizing nonadditive effects of delocalization or resonance, and Herndon et al.⁵ concluded that including these parameters improves the accuracy of $\Delta_f H^\circ$ predictions for polycyclic aromatic hydrocarbons (PAH) with three or more aromatic rings. A method for estimating ideal gas heat capacities has been proposed recently,⁶ which makes use of a single parameter, the ratio between the number of atoms in the molecule and its molar mass: since in the present work we deal with isomers of

Scheme 1. Simplified Reaction Pathway for 1-Methylnaphthalene Hydroconversion^a



^aHydrocracking reactions are omitted except for ring opening. Naphthalene is also produced by demethylation of 1-methylnaphthalene. Reaction numbers are in parentheses; compounds are numbered in bold.

compounds having very similar molar masses and compositions, we have preferred to use the older Benson method with structural contributions up to the third order, as a reference calculation to be compared with quantum chemical models.

Quantum chemical models coupled to statistical mechanics can approach experimental accuracies for molecular properties. However, polycyclic aromatics exhibit strongly correlated and extended π electrons systems, which are challenging for theory. Post Hartree–Fock methods are very accurate but computationally expensive.

Density Functional Theory (DFT) based methods on the other hand are computationally cheaper, but some functionals (like the popular B3LYP⁷) give a serious overestimation of the enthalpies of formation with respect to the experimental values.⁸ A systematic increase in the deviation with an increasing number of carbon atoms in a molecule has been reported by Van Speybroeck et al. at the B3LYP6-31G(d)/level.⁹ Composite methods (e.g., Gn-methods, G3B3, CBS-QB3) combine the results of several calculations, allowing more accurate estimation of heats of formation than DFT based methods.

In particular, the G4 theory has proven to be one of the most advanced methods to obtain accurate absolute energies.¹⁰ However, we are interested in reaction energies and not absolute energies. In order to compare the precision of *ab initio* methods with the group-based method of Benson, we have calculated the heats of formation of all compounds and compared them to experimental values when possible. We will present different methods to compute the heat of formation, using atomization energies of iso- and homodesmotic reactions. Isodesmic reactions conserve the number of types of bonds, while in homodesmotic reactions the hybridization of atoms in bonds is also conserved.¹¹ This type of reaction scheme aids in rescinding some of the systematic errors that arise in quantum mechanics, due to an incomplete capture of electronic correlation.^{12,13} However, since different isodesmic/homodesmotic reactions can be set up for the molecule of interest, the calculated thermodynamic property may be reaction dependent, as we will see later on.

In the next section, we detail the applied computational methods. We then discuss the obtained equilibrium constants from the computations and compare them with available experimental data where possible. To test the viability of our

Table 1. Experimental Data Available for S° , $\Delta_f H^\circ$, and $\Delta_f G^\circ$ at 298 K^a

molecule ^b	S° (J·mol ⁻¹ ·K ⁻¹)	$\Delta_f H^\circ$ (kJ·mol ⁻¹)	$\Delta_f G^\circ$ (kJ·mol ⁻¹)
1 (hydrogen)	130.6	0.0	0.0
2	377.5	116.9	217.9
3			
4	380.2	-7.9	170.3
5			
6	380.0	116.1	216.3
7			
8			
9			
10	333.2	150.6	224.1
11	413.7	79.9	211.0
12	369.6	26.6	167.1
13	374.6	-182.2	73.6
14	388.6	37.1	172.1
15	433.7	-21.6	138.8
16			
17			
18			
19	479.1	-33.8	153.6
20			
21			
22	483.0 ^c	-42.7 ^c	
23	490.0 ^c	-246.2 ^c	
24	477.0 ^c	-42.7 ^c	
25	490.0 ^c	-246.2 ^c	

^aThe experimental values were taken from the DIPPR database unless mentioned otherwise. ^bThe compounds numbered in bold are represented in Scheme 1. ^cValues taken from NIST database.¹⁵

model, i.e., the completeness of the reaction scheme presented in Scheme 1 and the accuracy of the computed data, we use the calculated thermodynamic data from Flash calculations in order to predict the final product composition under experimental reaction conditions and compare them with experiments by Bouchy et al., who studied the hydrogenation and hydrocracking of a model light cycle oil feed.²

METHODS

The experimental data used in this study were obtained from the DIPPR database¹⁴ and NIST database.¹⁵

Benson's GA method was used to estimate the heats of formation ($\Delta_f H^\circ$), entropy (S°), and heat capacity (C_p°) of all the molecules presented in Scheme 1.

For DFT calculations, the Jaguar package¹⁶ from Schrödinger was used, and the input structures were generated using Maestro.¹⁷ Geometry optimization calculations were performed at the B3LYP/6-31G(d,p) level with frequency calculations that use the harmonic oscillator approach. The resulting geometries at the B3LYP level were used as input structures for the Gaussian-4 (G4)¹⁸ composite method calculations with Gaussian 09.¹⁹

An atomization approach (eq 1) can be used to calculate the heat of formation and entropy of $C_n H_m$ from DFT calculations, as shown in the eqs 2 and 3. Equation 2 is visualized in Figure 1.



$$\begin{aligned} \Delta_f H^\circ(C_n H_m, 298K) &= n\Delta_f H_{\text{exp}}^\circ(C_{298K}) + m\Delta_f H_{\text{exp}}^\circ(H_{298K}) \\ &\quad - [nH_{\text{calc}}^\circ(C_{298K}) + mH_{\text{calc}}^\circ(H_{298K}) \\ &\quad - H_{\text{calc}}^\circ(C_n H_m, 298K)] \end{aligned} \quad (2)$$

$$\begin{aligned} S^\circ(C_n H_m, 298K) &= nS_{\text{exp}}^\circ(C_{298K}) + mS_{\text{exp}}^\circ(H_{298K}) \\ &\quad - [nS_{\text{calc}}^\circ(C_{298K}) + mS_{\text{calc}}^\circ(H_{298K}) \\ &\quad - S_{\text{calc}}^\circ(C_n H_m, 298K)] \end{aligned} \quad (3)$$

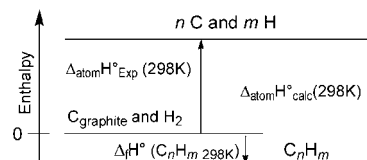


Figure 1. Illustration of the calculation of standard heats of formation from *ab initio* standard heats of atomization.

Important systematic errors in B3LYP and G4 calculations have been reported that result in deviations observed with respect to experimental enthalpies and entropies of carbon and hydrogen atoms. An overestimation of 30 kJ·mol⁻¹ with respect to the experimental values of the heats of formation was observed by Saeys et al.⁸ at the B3LYP/6-31G(d) level. The underestimation of atomization energies and the overestimation of enthalpies of formation using the B3LYP functional are due to the underestimation of the bond energies.⁹

Therefore, a different approach was used in parallel. In this approach, we establish the “real” reactions for the enthalpy of formation by taking experimental values, and eq 1–3 were modified as follows:



$$\begin{aligned} \Delta_f H^\circ(C_n H_m, 298K) &= n\Delta_f H_{\text{exp}}^\circ(C_{298K}) \\ &\quad + \frac{m}{2}\Delta_f H_{\text{exp}}^\circ(H_{2,298K}) \\ &\quad - \left[nH_{\text{calc}}^\circ(C_{298K}) + \frac{m}{2}H_{\text{calc}}^\circ(H_{2,298K}) \right. \\ &\quad \left. - H_{\text{calc}}^\circ(C_n H_m, 298K) \right] \end{aligned} \quad (5)$$

$$\begin{aligned} S^\circ(C_n H_m, 298K) &= nS_{\text{exp}}^\circ(C_{298K}) + \frac{m}{2}S_{\text{exp}}^\circ(H_{2,298K}) \\ &\quad - \left[nS_{\text{calc}}^\circ(C_{298K}) + \frac{m}{2}S_{\text{calc}}^\circ(H_{2,298K}) \right. \\ &\quad \left. - S_{\text{calc}}^\circ(C_n H_m, 298K) \right] \end{aligned} \quad (6)$$

For this approach, the following experimental data were used for carbon at 298.15 K: $\Delta_f H^\circ = 716.7$ kJ·mol⁻¹ and $S^\circ = 158.1$ J·mol⁻¹·K⁻¹.¹⁵ The experimental data for H₂ are shown in Table 1. For comparison, the heat of formation and entropy were also calculated using the atomization approach but values are not shown here; parity plots for this approach are provided in the Supporting Information (SI), Figures S1 and S2.

Flash calculations were carried out taking into account liquid–vapor equilibrium, which means that it is necessary to

calculate the equilibrium constants for each reaction. These constants can be calculated as follows:

$$K_{p,j}^{\circ}(T) = \exp\left(\frac{-\Delta_R G_j^{\circ}(T)}{RT}\right) = \prod_i (\hat{a}_i)^{\nu_{i,j}} \quad (7)$$

where $K_{p,j}^{\circ}$ is the equilibrium constant, R is the universal ideal gas constant, T is the temperature, \hat{a}_i is the activity for the component i , ν is the stoichiometry number, j represents the reaction number, and $\Delta_R G_j^{\circ}(T)$ is the change in the Gibbs energy for a reaction.

In order to calculate $\Delta_R G^{\circ}(T)$, we used the thermodynamic data calculated by the methods presented above. In the case of Benson's GA method, an extrapolation was made in order to calculate the thermodynamic properties at higher temperatures (above 298 K), using eqs 8 and 9.

$$\Delta H^{\circ}(T) = \Delta H^{\circ}(298 \text{ K}) + \int_{298\text{K}}^T C_p^{\circ}(T) dT \quad (8)$$

$$S^{\circ}(T) = S^{\circ}(298 \text{ K}) + \int_{298\text{K}}^T \frac{C_p^{\circ}(T)}{T} dT \quad (9)$$

where $C_p^{\circ}(T)$ is the polynomial form of constant pressure heat capacity.

$\Delta_R G^{\circ}(T)$ was calculated using the enthalpy and entropy as follows:

$$\Delta_R G^{\circ}(T) = \Delta H^{\circ}(T) - TS^{\circ}(T) \quad (10)$$

In the case of *ab initio* models, DFT calculations were carried out directly at the temperature desired.

Activities at equilibrium in the liquid and gas phase were calculated using the Peng–Robinson equation of state. If component i is present in the liquid phase, the activity is represented as

$$\hat{a}_i = x_i \frac{P\phi_i^l(T, P, x_i)}{P^{\circ}} \quad (11)$$

But, if component i is in the gas phase, the activity is calculated as

$$\hat{a}_i = y_i \frac{P\phi_i^v(T, P, y_i)}{P^{\circ}} \quad (12)$$

where P° is the pressure under standard conditions, i.e., 1 bar, and ϕ_i^l and ϕ_i^v are the fugacity coefficients in the liquid and gas phase, respectively.

The parameters of the Peng–Robinson equation of state are expressed in terms of the critical properties and the acentric factor; this information is reported in the 2011 version of the DIPPR 801 database (BYU DIPPR Lab).¹⁴ The critical properties not reported in this database can be obtained by the group contribution model proposed by Marrero and Gani.²⁰ The acentric factor (ω) was estimated by using the method proposed by Constantinou et al.²¹ The interaction parameters k_{ij} for hydrogen and hydrocarbon binaries were calculated by using the method proposed by Moysan and co-workers.²²

Fugacity coefficients depend on the final composition of the system, which is initially unknown, and a trial-and-error iterative method is required to calculate fugacity coefficients as well as the final composition. The criteria of mass balance by elements must be fulfilled. The SIMPLEX method²³ is used to minimize the error between the thermodynamic equilibrium

constants calculated using the Gibbs energy and those calculated in terms of activities (calculated using the equation of state). In order to achieve the calculation coupling phase and chemical equilibria, a first free energy minimization loop under mass balances constraints assuming a single gas phase is implemented; then a flash calculation is achieved and confirmed by a stability analysis in order to get a first guess of the amount of liquid phase if any; a second free energy minimization loop under constraints taking the gas and liquid phases into account allows one to predict the composition of both phases at equilibrium. Details of this algorithm have been published by Mougin et al.²⁴

RESULTS AND DISCUSSION

The gas phase standard state entropies and heats of formation (S° and $\Delta_f H^{\circ}$) have been calculated using Benson's GA method and QM methods at the B3LYP and G4 levels for all the compounds present in Table 1, and a comparison of the calculated values and experimental data is represented in Figure 2 (for $\Delta_f H^{\circ}$) and Figure 3 (for S°). See also Tables S1 and S2 in the Supporting Information, which also give examples of calculations using Benson's GA method.

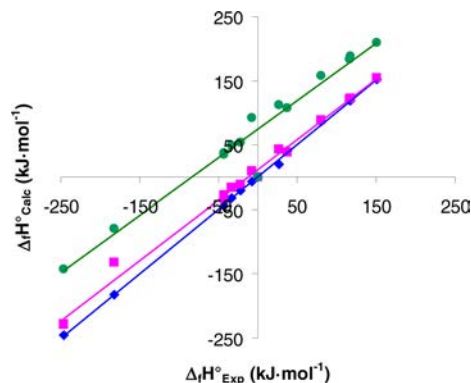


Figure 2. Parity plot for $\Delta_f H^{\circ}$: (◆) Benson, (■) G4, (●) B3LYP. Linear regression ($y = mx + b$): Benson: $m = 1.004$, $R^2 = 0.999$. B3LYP: $m = 0.892$, $b = 74.962$, $R^2 = 0.962$. G4: $m = 0.939$, $b = 11.743$, $R^2 = 0.993$.

In the case of the standard heat of formation, the linear regression for these models (Benson, B3LYP, and G4) shows

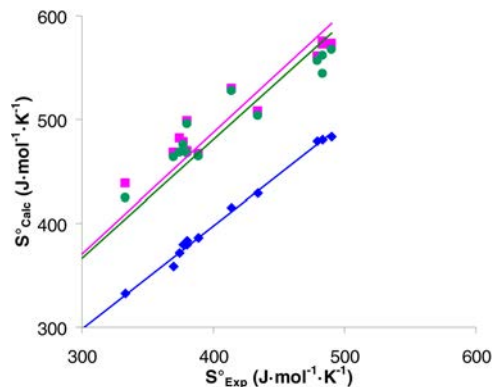
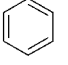
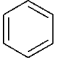
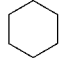
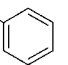
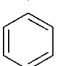
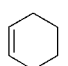


Figure 3. Parity plot for standard entropy (S°): (◆) Benson, (■) G4, (●) B3LYP. Linear regression ($y = mx + b$): Benson: $m = 0.994$, $R^2 = 0.998$. B3LYP: $m = 1.148$, $b = 22.182$, $R^2 = 0.954$. G4: $m = 1.174$, $b = 18.562$, $R^2 = 0.956$.

Table 2. S° , $\Delta_f H^\circ$, and $\Delta_f G^\circ$ Calculated by HI-G4-iso Method Using Different Iso/Homodesmotic Reactions for Tetralin as Compared to the Experimental Values of $S^\circ = 369.6 \text{ J}\cdot\text{mol}^{-1}\cdot\text{K}^{-1}$, $\Delta_f H^\circ = 26.61 \text{ kJ}\cdot\text{mol}^{-1}$, and $\Delta_f G^\circ = 167.1 \text{ kJ}\cdot\text{mol}^{-1}$

	Homodesmotic Reaction	$S^\circ \text{ (J}\cdot\text{mol}^{-1}\cdot\text{K}^{-1})$	$\Delta_f H^\circ \text{ (kJ}\cdot\text{mol}^{-1})$	$\Delta_f G^\circ \text{ (kJ}\cdot\text{mol}^{-1})$
a	+ 12CH ₄ → 8C ₂ H ₆ + 3C ₂ H ₄	255.5	28.3	136.9
b	+ 2CH ₄ →  + C ₆ H ₁₄	285.6	28.2	155.9
c	+ C ₂ H ₆ →  + 	337.5	28.8	174.8
d	+ 2CH ₄ →  + C ₅ H ₁₂	298.1	27.8	156.1
e	+ C ₂ H ₄ →  + 	360.6	28.4	168.3

an overestimation of $\Delta_f H^\circ$ by B3LYP, while a good ($R^2 = 0.990$) to excellent ($R^2 = 0.999$) agreement is found for, respectively, G4 and Benson.

Benson's method also calculates the entropy more accurately than B3LYP or G4 (Figure 3). For the QM calculations, the entropy contributions are calculated from the partition functions that use frequencies that were evaluated from the relaxed structure obtained at the B3LYP/6-31G(d,p) level and in the case of the G4 calculations at the B3LYP/6-31G(2df,p) level. The small difference between the two methods explains why the results for the entropy are that similar. The harmonic oscillator approximation is used in the assessment of the vibrational frequencies. This approximation might no longer be sufficiently precise for molecules with a large degree of flexibility and a high number of rotatable groups.⁹ The shape of the rotational energy curve can give rise to various stable conformers for the investigated molecules. Furthermore, the presence of rotatable groups in the molecule can cause the wrong assignment of the symmetry number of the molecule, thereby introducing serious errors in the evaluation of the rotational entropy.

A remarkable improvement to calculate the Gibbs energy of formation and absolute entropies can be achieved by the utilization of isodesmic and homodesmotic reactions. However, the final results will depend on the choice of the homodesmotic reaction. This is, for example, illustrated in Table 2, where five different isodesmic reactions are given (of which four are homodesmotic) to calculate the thermodynamic properties of tetralin. Here, the total energy of tetralin is calculated at the G4 level, while experimental heats (or Gibbs energy) of formation and absolute entropies are used for the small molecules, e.g., methane, ethane, and cyclohexane. We refer to hybrid-improved-G4-iso (HI-G4-iso) if the absolute energies come from G4 calculations and hybrid-improved-B3LYP-iso (HI-B3LYP-iso) if they are calculated at B3LYP/6-31G(d,p).

One way to describe isodesmic reactions in a systematic way, is the "bond separation reaction" in which all formal bonds between non-hydrogen atoms are separated into the simplest parent molecules containing these same kinds of bonds. All other bonds to the desired atom pair are replaced by hydrogen atoms, and the chemical equation is balanced by including the required number of single heavy atom hydrides, i.e., methane for hydrocarbons. For example, tetralin would be described as reaction a in Table 2. Yet, this method suffers from the fact that a relatively small error in the heat of formation of methane can

produce a significant error in the heat of formation of 1-methyltetralin, due to a large number of methane molecules in equation a.²⁵ It thus turns out that this reaction relatively poorly describes the thermodynamical properties of tetralin.

The thermodynamic properties are better reproduced with homodesmotic reactions, e.g., reactions b–e in Table 2. Generally, the use of homodesmotic reactions improves the accuracy of the calculated properties, as observed as well by Sivaramakrishnan et al.²⁶ It was also noticed that the conservation of naphthenic rings ameliorates the precision of the calculated thermodynamic properties. We also noticed that the results for entropy were further improved if one olefin bond was introduced in the naphthenic cycle to introduce some kind of rigidity, if this ring is fused to an aromatic ring in the reactant, as for example reaction e in Table 2.

Figures 4 and 5 show parity plots for respectively $\Delta_f H^\circ$ and S° where the calculated values (Benson, HI-B3LYP-iso, and HI-

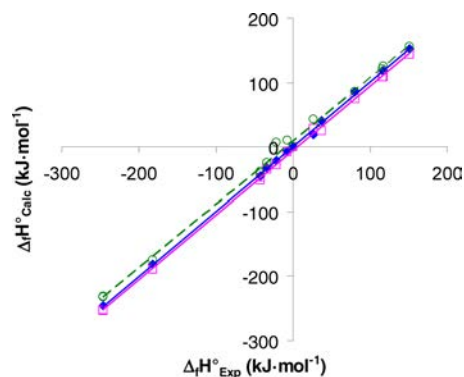


Figure 4. Parity plot for $\Delta_f H^\circ$: (◆) Benson, (□) HI-G4-iso, (○) HI-B3LYP-iso. Linear regression ($y = mx + b$): Benson: $m = 1.004$, $R^2 = 0.999$. HI-G4-iso: $m = 1.008$, $R^2 = 0.997$. HI-B3LYP-iso: $m = 0.982$, $b = 7.326$, $R^2 = 0.999$.

G4-iso) are compared to experimental data. The use of homodesmotic reactions has significantly improved the accuracy of the calculated properties. This is also illustrated in Tables 3 and 4, where the absolute average relative deviation (AARE) and the root-mean-square error (RMSE) have been reported for $\Delta_f H^\circ$ and S° . From these tables, it follows that Benson's GA empirical model has the smallest deviation for $\Delta_f H^\circ$ and S° , while among quantum chemical models, HI-G4-iso reproduces better both $\Delta_f H^\circ$ and S° experimental values.

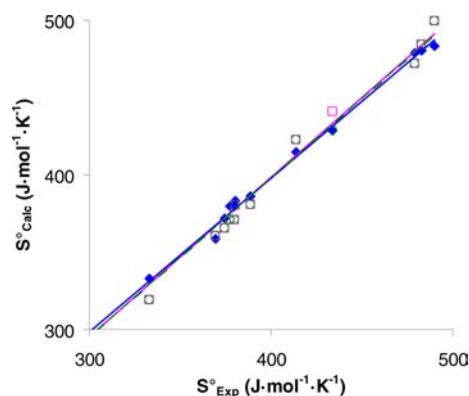


Figure 5. Parity plot for standard entropy (S°): (◆) Benson, (□) HI-G4-iso, (○) HI-B3LYP-iso. Linear regression ($y = mx + b$): Benson: $m = 0.994$, $R^2 = 0.998$. HI-G4-iso: $m = 1.024$, $b = -12.522$, $R^2 = 0.992$. HI-B3LYP-iso: $m = 1.048$, $b = -25.204$, $R^2 = 0.961$.

Table 3. Deviation of the $\Delta_r H^\circ$ Predicted by Different Methods to the Experimental Data Available for $\Delta_r H^\circ$ in $\text{kJ}\cdot\text{mol}^{-1}$

	$\Delta_r H^\circ$				
	Benson	B3LYP	HI-B3LYP-iso	G4	HI-G4-iso
AARE (%)	6.2	237.0	28.9	38.2	10.4
RMSE	2.9	78.9	8.8	17.4	6.3

Table 4. Deviation of the S° Predicted by Different Methods to the Experimental Data Available for S° in $\text{J}\cdot\text{mol}^{-1}\cdot\text{K}^{-1}$

	S°				
	Benson	B3LYP	HI-B3LYP-iso	G4	HI-G4-iso
AARE (%)	0.8	21.3	1.7	23.1	1.8
RMSE	4.3	85.3	7.7	92.2	7.8

Additionally, HI-G4-iso is completely universal, while Benson's method is not.

The equilibrium constant for a given process or reaction can be expressed in terms of Gibbs energy (see eq 7). This property ($\Delta_r G_{673\text{K}}^\circ$) was calculated by using Benson's model and the QM models (G4, B3LYP, HI-B3LYP-iso, and HI-G4-iso) for each reaction present in Scheme 1. Figure 6 shows a comparison

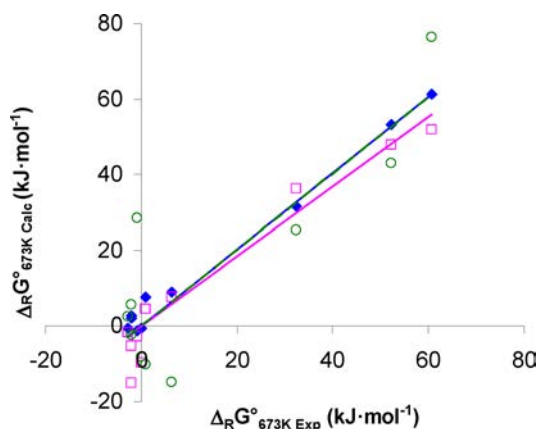


Figure 6. Parity plot for Gibbs energy estimation at 673K ($\Delta_r G_{673\text{K}}^\circ$): (◆) Benson, (□) HI-G4-iso, (○) HI-B3LYP-iso. Linear regression ($y = mx$): Benson: $m = 1.007$, $R^2 = 0.980$. HI-G4-iso: $m = 0.92$, $R^2 = 0.935$. B3LYP-iso: $m = 1.005$, $R^2 = 0.735$.

between those models (Benson, HI-G4-iso, and HI-B3LYP-iso models) and experimental data available, and Table 5 shows the deviation of calculated values from experimental data.

Table 5. Deviation of the $\Delta_r G_{673\text{K}}^\circ$ Predicted by Different Methods from the Experimental Data Available for $\Delta_r G_{673\text{K}}^\circ$ in $\text{kJ}\cdot\text{mol}^{-1}$

	$\Delta_r G_{673\text{K}}^\circ$ ($\text{kJ}\cdot\text{mol}^{-1}$)				
	Benson	B3LYP	HI-B3LYP-iso	G4	HI-G4-iso
RMSE	3.2	10.1	14.0	9.4	6.4
bias	-2.0	4.9	-0.1	-4.7	3.1

A smaller dispersion for $\Delta_r G_{673\text{K}}^\circ$ was observed for Benson's model (confirmed by a slope close to 1 for Benson's model), but errors of the same magnitude were obtained by using the HI-G4-iso model. Significant improvement was obtained by using DFT models with isodesmic reactions, especially at the G4 level, where the RMSE is reduced from 9.4 to 6.4.

The smallest deviations for $\Delta_r H^\circ$ and S° are obtained for Benson's model. However, remember that Benson's GA method cannot always distinguish between position isomers observed in the hydroconversion process. Nonetheless, HI-G4-iso could allow filling this gap, to estimate the equilibrium constant for isomerization reactions if experimental data are not available for position isomers.

Product Composition Prediction. In order to validate the methods studied, Benson's model and the HI-G4-iso method were chosen to estimate the equilibrium constant for the reactions represented in Scheme 1. Flash calculations were made to determine the equilibrium state for 1-methylnaphthalene hydroconversion at 40 bar and 400 °C.

Experimental results obtained by Bouchy et al.²⁷ under these conditions (40 bar and 400 °C) suggest a thermodynamic equilibrium for the (direct) hydrogenation reactions of 1MN. The discrepancy between the experimental 2MN/1MN ratio of about 0.17 and the theoretical value of 1.5 at thermodynamic equilibrium clearly demonstrate that isomerization reaction (5) is kinetically limited. Since the catalytic system does not contain any (strong) acid sites to catalyze this reaction, this reaction becomes kinetically prohibited, thereby explaining the much lower ratio experimentally observed.

However, in the flash calculations, which assume thermodynamic equilibrium for all reactions, the products related to this isomerization reaction (as well as other isomerization reactions and cracking reaction that are acid-catalyzed) thus will be overestimated with respect to the experimental values. This is shown in Table 6, in which hydrogenation and conversion were calculated as follows:

$$\begin{aligned} \text{hydrogenation 1MN (\%)} \\ = 100(1 - X_2 - X_6 - X_{10} - X_{11}) \end{aligned} \quad (13)$$

$$\text{conversion (\%)} = 100(1 - X_2 - X_6) \quad (14)$$

To remedy this discrepancy, we have simplified the reaction pathway (Scheme 1) by omitting the isomerization and cracking reactions, focusing exclusively on hydrogenation of the first and second rings of 1MN (reactions 1–4, as shown in Figure 7). By taking into account only the hydrogenation reactions, it follows that Benson's GA method better reproduces the experimental data of Bouchy than HI-G4-iso.

Table 6. Flash Calculation Results at 40 bar and 400 °C Compared to Empirical Data

molecule	liquid composition (% mol)		
	Benson	HI-G4-iso	exptl. ^a
2	1.55	0.08	37.90
6	1.75	0.11	6.30
3	0.95	0.05	22.20
4	0.10	0.01	9.80
7	0.11	0.04	1.60
9	0.94	0.26	3.70
20	0.60	0.01	
5 + 8	0.34	0.05	5.20
21	0.04	0.08	
16	0.09	0.81	1.50
18	0.12	0.09	0.50
14	1.58	0.04	
17 +19	5.90	1.86	2.7
15	20.38	6.23	
22 + 24	52.23	78.91	0.5
23 + 25	9.67	11.04	0.1
12	1.05	0.02	1.70
13	0.46	0.04	
10	0.34	0.01	1.20
11	1.81	0.27	1.10
hydrogenation 1MN (%)	94.6	99.5	49.5
conversion (%)	96.7	99.8	55.8

^aThe experimental values were taken from Bouchy et al.²⁷

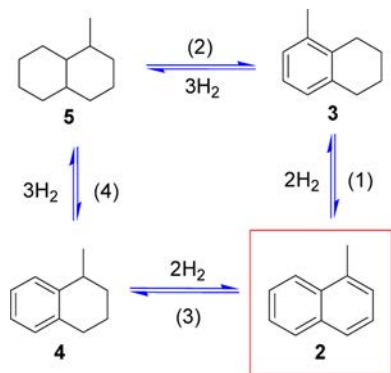


Figure 7. Hydrogenation of the first and second aromatic rings of 1MN.

Results from this calculation are shown in Table 7. Calculated values using Benson’s GA method are in good agreement with experimental results obtained by Bouchy et al. (an error around 5%).

The poorer agreement of the HI-G4-iso method can be explained by the differences observed for equilibrium constants values. Table 8 shows the equilibrium constants calculated at 673 K for Benson’s and HI-G4-iso methods. Bouchy et al.²⁷ reported an equilibrium constant of 9.4×10^{-4} for reaction 1 and a value of 8.2×10^{-6} for reaction 2. This overestimation (or underestimation) of equilibrium constants is also observed by the overestimation of methyldecalin composition calculated using the HI-G4-iso method.

The integration of kinetic data in a microkinetic model that would use the rate constants for all essential elementary reactions would be a more elegant way to describe these experiments. These kinetic data can be obtained from experiments or by quantum mechanical calculations. The ratios

Table 7. Compositions Obtained from Flash Calculations at 40 bar and 400 °C for 1MN Hydrogenation Compared to Empirical Data

	exptl. ^a	calculated	
		Benson	HI-G4-iso
X_{1MN}	0.52	0.54	0.44
X_{xMT}	0.40	0.39	0.33
X_{1MD}	0.07	0.07	0.23

^aThe experimental values were taken from Bouchy et al.²⁷ X_{1MN} , X_{xMT} , and X_{1MD} refer to the molar fractions of 1MN, 1-methyl and 5-methyltetralin, and *trans*-1-MD, respectively, with $X_{1MN} + X_{xMT} + X_{1MD} = 1$.

Table 8. Equilibrium Constants Calculated at 673 K

reaction	K_P°	
	Benson	HI-G4-iso
1	7.34×10^{-04}	6.70×10^{-04}
2	7.73×10^{-06}	3.66×10^{-05}
3	7.37×10^{-05}	1.94×10^{-04}
4	7.70×10^{-05}	1.27×10^{-04}

of direct and inverse kinetic constants should then be equal to equilibrium constants in order to satisfy the microreversibility principle. Therefore, the present work is a necessary first step allowing one to introduce consistently such constraints in the microkinetic model. We have started to explore if the rate constants from full DFT calculations and those that are incorporated in a microkinetic model are sufficiently precise to describe these experiments. Once we have identified the reactions that are most rate-limiting, we can make suggestions to fine-tune this reaction to the desired products. This will be the object of a future publication.

CONCLUSIONS

We report an assessment of various DFT models for the calculation of molecular thermochemical properties in comparison with Benson’s group contribution method for reactants, intermediates, and products involved in the hydrogenation of 1-methylnaphthalene. Parity plots are compared with reference to available experimental data.

For this particular set of structures, Benson’s GA method affords consistently the smallest deviations with respect to experimental data, reflecting the inherent correlative and interpolative nature of this method. Its prediction upon extrapolation to ill documented classes of structures will however remain questionable.

Among QM models, we have found HI-G4-iso, which combines evaluations of enthalpies and entropies of formation through improved homodesmotic schemes, as the most reliable, combining minimal RSME and bias.

Although small deviations are observed for $\Delta_f H^\circ$ and S° for Benson’s and HI-G4-iso methods, discrepancies were observed between experimental product composition and those obtained by a simple thermodynamic model. As mentioned above, depending on the catalyst properties, the observed distribution of products may be far from full thermodynamic equilibrium. It is well-known for instance that the completion of hydrocracking, hydroisomerization, and hydrodeacyclization reactions requires strong acid sites, together with sites able to activate hydrogenation and dehydrogenation reactions. Since acid sites were lacking in the experiments to which we referred, data

reconciliation was possible assuming a scheme strictly limited to the latter reactions. For the interpretation of experimental results in the general case, a comprehensive microkinetic model will be needed, including consistently the thermodynamics constraints. Our work was a first step toward the goal of establishing such a model from first principles.

ASSOCIATED CONTENT

Tables showing a compilation of available experimental data and estimated heats of formation (Table S1) and entropies (Table S2) for the set of molecules used in this study; a compilation of the estimated values using the atomization approach of standard heat of formation (Figure S1) and standard entropy (Figure S2); tables showing a compilation of experimental data available, isodesmic reactions, and estimated values at the HI-G4-iso level for the set molecules used in this study (Table S3); and estimated values at 673 K of Gibbs energy (Table S4) and equilibrium constants (Table S5) of reactions shown in Scheme 1. This material is available free of charge via the Internet at <http://pubs.acs.org>.

AUTHOR INFORMATION

Corresponding Author

*E-mail: herve.toulhoat@ifpen.fr.

Notes

The authors declare no competing financial interest.

ABBREVIATIONS

1MN = 1-methylnaphthalene

MT = methyltetralin

1MD = 1-methyldecalin

RMSE = root mean square error

AARE = absolute average relative error

$$\text{RMSE} = \sqrt{\sum_i^n \frac{(x_{i,\text{calculated}} - x_{i,\text{experimental}})^2}{n}}$$

$$\text{AARE} (\%) = \frac{100}{n} \cdot \sum_i^n \left| \frac{x_{i,\text{calculated}} - x_{i,\text{experimental}}}{x_{i,\text{experimental}}} \right|$$

$$\text{bias} = \sum_i^n \frac{x_{i,\text{calculated}} - x_{i,\text{experimental}}}{n}$$

REFERENCES

- (1) *Catalysis by Transition Metal Sulphides. From Molecular Theory to Industrial Application*; Toulhoat, H., Raybaud, P., Eds.; Editions Technip: Paris, 2013.
- (2) (a) Bouchy, M.; Dufresne, P.; Kasztelan, S. *Ind. Eng. Chem. Res.* **1993**, *32*, 1592–1602. (b) Miiki, Y.; Sugimoto, Y. *Fuel Process. Technol.* **1995**, *43*, 137–146. (c) McVicker, G. B.; Daage, M.; Touvelle, M. S.; Hudson, C. W.; Klein, D. P.; Baird, W. C., Jr.; Cook, B. R.; Chen, J. G.; Hantzer, S.; Vaughan, D. E. W.; Ellis, E. S.; Feeley, O. C. *J. Catal.* **2002**, *210*, 137–148. (d) Leininger, J.-P.; Lorant, F.; Minot, C.; Behar, F. *Energy Fuels* **2006**, *20*, 2518–2530. (e) Leininger, J.-P.; Lorant, F.; Minot, C.; Behar, F. *J. Phys. Chem. A* **2007**, *111*, 3082–3090. (f) Demirel, B.; Wiser, W. H. *Fuel Process. Technol.* **1998**, *55*, 83–91. (g) Yang, M.-G.; Nakamura, I.; Fujimoto, K. *Catal. Today* **1998**, *43*, 273–280.
- (3) (a) Verstraete, J. J.; Schnongs, Ph.; Dulot, H.; Hudebine, D. *Chem. Eng. Sci.* **2010**, *65*, 304–312. (b) Murgich, J.; Rodriguez, J.; Aray, Y. *Energy Fuels* **1996**, *10*, 68–76. (c) Suzuki, T.; Itoh, M.; Takegami, Y.; Watanabe, Y. *Fuel* **1982**, *61*, 402–410. (c) Gauthier, T.; Danial-Fortain, P.; Merdrignac, I.; Guibard, I.; Quoineaud, A.-A. *Catal. Today* **2008**, *130*, 429–438. (d) Takegami, Y.; Watanabe, Y.; Suzuki, T.; Mitsudo, T.; Itoh, M. *Fuel* **1980**, *59*, 253–259.
- (4) Benson, S. W.; Cruickshank, F. R.; Golden, D. M.; Haugen, G. R.; O'Neal, H. E.; Rodgers, A. S.; Shaw, R.; Walsh, R. *Chem. Rev.* **1969**, *69*, 279–324.
- (5) Herndon, W. C.; Biedermann, P. U.; Agranat, I. *J. Org. Chem.* **1998**, *63*, 7445–7448.
- (6) Dadgostar, N.; Shaw, J. M. *Fluid Phase Equilib.* **2013**, *344*, 139–151.
- (7) Becke, A. D. *J. Chem. Phys.* **1993**, *98*, 1372–1377.
- (8) Saeys, M.; Reyniers, M.-F.; Marin, G. B.; Van Speybroeck, V.; Waroquier, M. *J. Phys. Chem. A* **2003**, *107*, 9147–9159.
- (9) Van Speybroeck, V.; Gani, R.; Meier, R. J. *Chem. Soc. Rev.* **2010**, *39*, 1764–1779.
- (10) Curtiss, L. A.; Redfern, P. C.; Raghavachari, K. *Chem. Phys. Lett.* **2010**, *499*, 168–172.
- (11) McNaught, A. D.; Wilkinson, A. IUPAC. *Compendium of Chemical Terminology*, 2nd ed. (the “Gold Book”); Blackwell Scientific Publications: Oxford, U. K., 1997. XML on-line corrected version: <http://goldbook.iupac.org> (2006) created by Nic, M.; Jirat, J.; Kosata, B. Updates compiled by Jenkins, A. ISBN 0-9678550-9-8. DOI:10.1351/goldbook.
- (12) Yu, J.; Sumathi, R.; Green, W. H., Jr. *J. Am. Chem. Soc.* **2004**, *126*, 12685–12700.
- (13) Hehre, W. J.; Ditchfield, R.; Radom, L.; Pople, J. A. *J. Am. Chem. Soc.* **1970**, *92*, 4796–4801.
- (14) Rowley, R. L.; Wilding, W. V.; Oscarson, J. L.; Yang, Y.; Zundel, N. A.; Daubert, T. E.; Danner, R. P. *DIPPR Data Compilation of Pure Compound Properties*; Design Institute for Physical Property Data, AIChE: New York, 2003.
- (15) Afeefy, H. Y.; Liebman, J. F.; Stein, S. E. *Gaz Phase Thermochemical Data in NIST Chemistry WebBook, NIST Standard Reference Database Number 69*; Linstrom, P. J., Mallard, W. G., Eds.; National Institute of Standards and Technology: Gaithersburg, MD, 2011. <http://webbook.nist.gov>.
- (16) *Jaguar*, version 7.9; Schrödinger, LLC: New York, 2012.
- (17) *Maestro*, version 9.3; Schrödinger, LLC: New York, 2012.
- (18) Curtiss, L. A.; Redfern, P. C.; Raghavachari, K. *J. Chem. Phys.* **2007**, *126*, 084108.
- (19) Frisch, M. J.; Trucks, G. W.; Schlegel, H. B.; Scuseria, G. E.; Robb, M. A.; Cheeseman, J. R.; Scalmani, G.; Barone, V.; Mennucci, B.; Petersson, G. A.; Nakatsuji, H.; Caricato, M.; Li, X.; Hratchian, H. P.; Izmaylov, A. F.; Bloino, J.; Zheng, G.; Sonnenberg, J. L.; Hada, M.; Ehara, M.; Toyota, K.; Fukuda, R.; Hasegawa, J.; Ishida, M.; Nakajima, T.; Honda, Y.; Kitao, O.; Nakai, H.; Vreven, T.; Montgomery, J. A., Jr.; Peralta, J. E.; Ogliaro, F.; Bearpark, M.; Heyd, J. J.; Brothers, E.; Kudin, K. N.; Staroverov, V. N.; Keith, T.; Kobayashi, R.; Normand, J.; Raghavachari, K.; Rendell, A.; Burant, J. C.; Iyengar, S. S.; Tomasi, J.; Cossi, M.; Rega, N.; Millam, J. M.; Klene, M.; Knox, J. E.; Cross, J. B.; Bakken, V.; Adamo, C.; Jaramillo, J.; Gomperts, R.; Stratmann, R. E.; Yazyev, O.; Austin, A. J.; Cammi, R.; Pomelli, C.; Ochterski, J. W.; Martin, R. L.; Morokuma, K.; Zakrzewski, V. G.; Voth, G. A.; Salvador, P.; Dannenberg, J. J.; Dapprich, S.; Daniels, A. D.; Farkas, O.; Foresman, J. B.; Ortiz, J. V.; Cioslowski, J.; Fox, D. J. *Gaussian 09*, Revision B.01; Gaussian, Inc.: Wallingford, CT, 2010.
- (20) Marrero, J.; Gani, R. *Fluid Phase Equilib.* **2001**, *183–184*, 183–208.
- (21) Constantinou, L.; Gani, R.; O'Connell, J. P. *AIChE J.* **1995**, *103*, 11–22.
- (22) Moysan, J. M.; Huron, M. J.; Paradowski, H.; Vidal, J. *Chem. Eng. Sci.* **1983**, *38*, 1085–1092.
- (23) Nelder, J. A.; Mead, R. *Comput. J.* **1965**, *7*, 308–313.
- (24) Mougín, P.; Lamoureux-Var, V.; Bariteau, A.; Huc, A. Y. *J. Petrol. Sci. Eng.* **2007**, *58*, 413–427.
- (25) Petersson, G. A.; Malick, D. K.; Wilson, W. G.; Ochterski, J. W.; Montgomery, J. A.; Frisch, M. J. *J. Chem. Phys.* **1998**, *109*, 10570–10579.
- (26) Sivaramakrishnan, R.; Tranter, R.; Brezinsky, K. *J. Phys. Chem. A* **2005**, *109*, 1621–1628.
- (27) Bouchy, M.; Dufresne, P.; Kasztelan, S. *Ind. Eng. Chem. Res.* **1992**, *31*, 2661–2669.